

Welche globale Erwärmung? 148 neue (2020) wissenschaftliche Studien bestätigen, dass es in letzter Zeit keine Erwärmung gab...

geschrieben von Chris Frey | 19. Januar 2021

Der Link zur Datengrundlage der im Jahre 2020 (und 2019) veröffentlichten Studien, welche belegen, dass es keine globale Erwärmung gab, ist hier:

Non-Global Warming Studies From 2020 & 2019

Es folgen 8 Beispiele der im Jahre 2020 veröffentlichten 148 Studien zur fehlenden globalen Erwärmung:

Martin et al., 2020: Die maximale Temperatur im Holozän in Frankreich (14°C) lagen um 7 K über dem heutigen Wert (7°C)

„Moderne Klimaparameter wurden aus der instrumentellen Datenbank von Meteo-France an der 11 km entfernten Station Mazet-Volamont (1130 m) für den Zeitraum 2009-2017 gewonnen ... Die Temperaturwerte wurden mit einem vertikalen Temperaturgradienten von 0,6°C/100 m korrigiert. Die mittleren Jahrestemperaturen variieren zwischen 6 und 9°C mit einem Mittelwert von 7°C. ... Die mittlere Jahrestemperatur für das gesamte Holozän betrug 11,3°C, d.h. Sie lag um 4,1°C über dem modernen Wert. Das Maximum von 14°C und ein Minimum von 7,6°C wurden vor 7800 bzw. 1700 Jahren erreicht. ... Die letzten 200 Jahre zeigen einen gegenläufigen Trend ... MAAT sank um 3,1 und 3,3°C für die Seekalibrationen, Sun et al. (2011) und Russell et al. (2018), bzw. 2,1°C für die Bodenkalisierung.“



Early Holocene Thermal Maximum recorded by branched tetraethers and pollen in Western Europe (Massif Central, France)

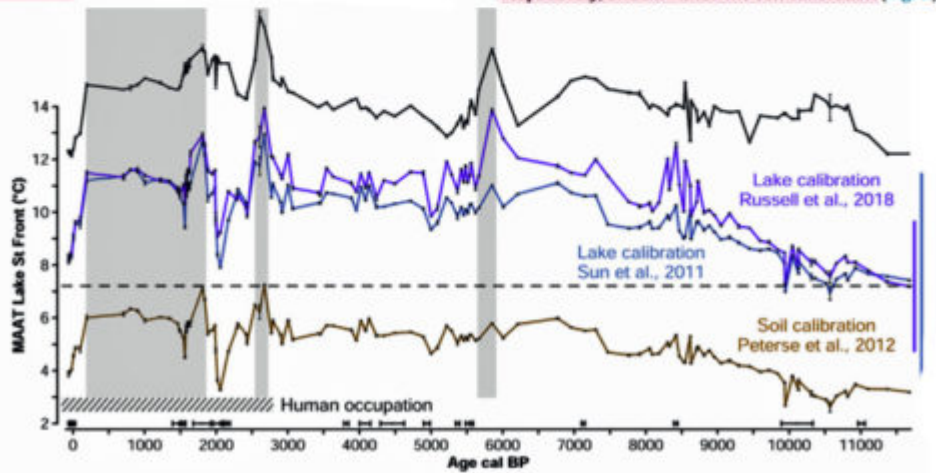
Céline Martin^{a,b,*}, Guillemette Ménot^{a,c,d}, Nicolas Thouveny^a, Odile Peyron^a, Valérie Andrieu-Ponel^e, Vincent Montade^{a,c}, Nina Davtian^a, Maurice Ralle^f, Edouard Bard^a

Lake St Front lies on the Meygal-Mézenc plateau in the eastern Velay in the Massif Central, France (44°58' lat N; 4°10' long E; 1234 m, Fig. 1A).

Modern climatic parameters were obtained from the instrumental database of Météo-France (<https://donneespubliques.meteofrance.fr>) at the nearby station of Mazet-Volamont (1130 m) located 11 km distant, for the period 2009–2017, and for longer data series, at the stations of Saint Julien Chaptueil (distance 9 km, altitude 810 m, period 1995–2017) and Le Puy en Velay (distance 22 km, altitude 833 m, period 1981–2010, Fig. 1C). Temperature values were corrected using a lapse rate of 0.6 °C/100 m. Mean annual temperatures vary between 6 and 9 °C with a mean value of 7 °C.

The mean annual temperature for the entire Holocene was 11.3 °C, i.e. 4.1 °C above the modern value. The maximum of 14 °C and a minimum of 7.6 °C were reached, respectively, at 7.8 and 1.7 kyr cal BP. The annual temperatures increased abruptly from 10.6 to 9.8 kyr cal BP then remained high until 7.4 kyr cal BP. The period between 7.4 and 6 kyr cal BP is marked by a cooling event, but the annual temperatures rose again at 6 kyr cal BP prior to decreasing regularly until 2 kyr cal BP and then oscillating around a mean value of 9.2 °C (Fig. 4B). The MTWA also showed a rapid increase from 10.6 to 10 kyr cal BP (+2.7 °C) then temperatures continued increasing until 7.4 kyr cal BP prior to a decrease until around 3.5 kyr cal BP and stabilizing around 17.7 °C with numerous rapid oscillations (Fig. 4C).

Through the Holocene, the $\Sigma\text{IIIa}/\Sigma\text{IIa}$ ratio showed a general decreasing trend (from 1.2 to 0.6, Fig. 2A, Sup Table 5) while the MBT, MBT', MBT'_{SMe} and CBT indices increased through the Holocene (from 0.17 to 0.29, 0.17 to 0.3, 0.26 to 0.39 and 0.52 to 0.71 respectively, Fig. 2B–D). The reconstructed mean annual air temperatures (MAAT) followed the same increasing trend (Fig. 2E). Using the lacustrine calibrations the MAAT increased from 7.4 to 11.2 °C and from 7.2 to 11.5 °C with a maximal amplitude of 6 and 6.7 °C with the Sun et al. (2011) and Russell et al. (2018) calibrations, respectively (Fig. 2E). The soil calibration of Peterse et al. (2012) led to an increase from 3.2 to 6 °C with a maximal amplitude of 4.6 °C (Fig. 2E). The last 200 years display an opposite trend: the $\Sigma\text{IIIa}/\Sigma\text{IIa}$ ratio increased by 0.26, the MBT, MBT' and MBT'_{SMe} decreased by 0.1 and CBT by 0.2. MAAT decreased by 3.1 and 3.3 °C for the lake calibrations, Sun et al. (2011) and Russell et al. (2018), respectively, and 2.1 °C for the soil calibration (Fig. 2).



Mean annual air temperatures (MAAT) reconstructed with Sun et al. (2011, blue curve), Russell et al. (2018, purple curve) and Peterse et al. (2012, brown curve) calibrations compared with the present mean annual temperature at St Front (black dashed line)

Hou et al., 2020: Der westliche tropische Atlantik war um 1 bis 5 K wärmer während der letzten Eiszeit (CO₂-Gehalt 190 ppm)

Unsere Ergebnisse zeigen einen Mangel an ausgeprägter glazial-interglazialer Variabilität in der SST-Aufzeichnung, was uns dazu veranlasst, atmosphärischen pCO₂ als direkten Treiber der SST-Variationen im südlichen WTA [westlicher tropischer Atlantik] auszuschließen.



Forcing of western tropical South Atlantic sea surface temperature across three glacial-interglacial cycles

Alicia Hou^{a,*}, André Bahr^a, Stefan Schmidt^a, Cornelia Strebl^a, Ana Luiza Albuquerque^b, Cristiano M. Chiessi^c, Oliver Friedrich^a

The western tropical Atlantic (WTA) supplies warm and saline waters to the upper-limb of the Atlantic Meridional Overturning Circulation (AMOC) and may store excess heat and salinity during periods of AMOC slowdown. Since previous sea surface temperature (SST) reconstructions from the WTA typically focus on the Last Glacial Maximum and the last deglaciation, additional long-term records spanning multiple glacial-interglacial transitions are needed in order to elucidate the drivers of long-term WTA SST variability. We performed Mg/Ca analyses on the surface-dwelling planktic foraminifera *Globigerinoides ruber* (pink) from a sediment core raised from the southern WTA to reconstruct SST changes over the past 322 kyr. We evaluate the relative importance of atmospheric $p\text{CO}_2$, AMOC strength and trade-wind intensity in driving the thermal evolution of the WTA across three glacial-interglacial cycles. Our results indicate a lack of pronounced glacial-interglacial variability in the SST record, prompting us to exclude atmospheric $p\text{CO}_2$ as a direct driver of SST variations in the southern WTA.

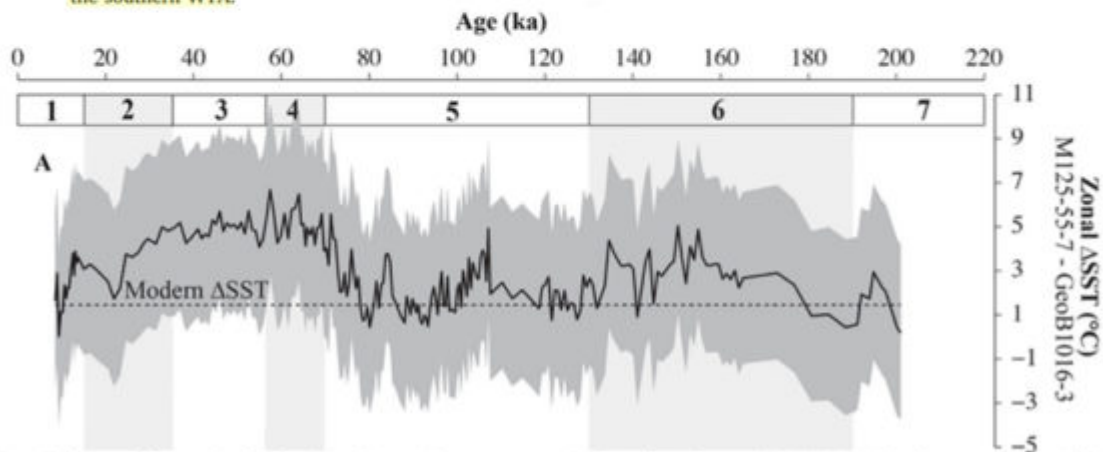


Fig. 5. Monte Carlo ensemble mean South Atlantic zonal sea surface temperature (SST) gradients between Site M125-55-7 (southern western tropical Atlantic) and Sites GeoB1016-3 and GeoB1028-5 located in the eastern (sub)tropical South Atlantic (Sites 3 and 4 in Fig. 1; Schneider et al., 1995). (A) Monte Carlo ensemble mean SST gradient between sites M125-55-7 and GeoB1016-3 (black line). The grey shading represents the 95% confidence envelope.

Xia et al., 2020: Die Sommertemperatur im subantarktischen Georgien „lag um 5 bis 10 K höher als heute“

Obwohl der Biomarker-basierte Paläo-Temperatur-Proxy für moderne Temperaturdaten regionaler Seen kalibriert wurde, liegen die aus dem Fan Lake rekonstruierten Sommertemperaturen bis zu 14°C außerhalb des Bereichs ihres modernen Kalibrierungsdatensatzes, in dem der wärmste Standort eine Sommertemperatur von nur 10°C aufweist (Foster et al., 2016) ... Die CARs stiegen auf bis zu 140 g C pro m^2 und Jahr vor 4000 bis 3500 Jahren und 70 g C pro m^2 und Jahr vor 3200 bis 2700 Jahren, als die Sommertemperatur um etwa 10°C bzw. 5°C höher war als heute.



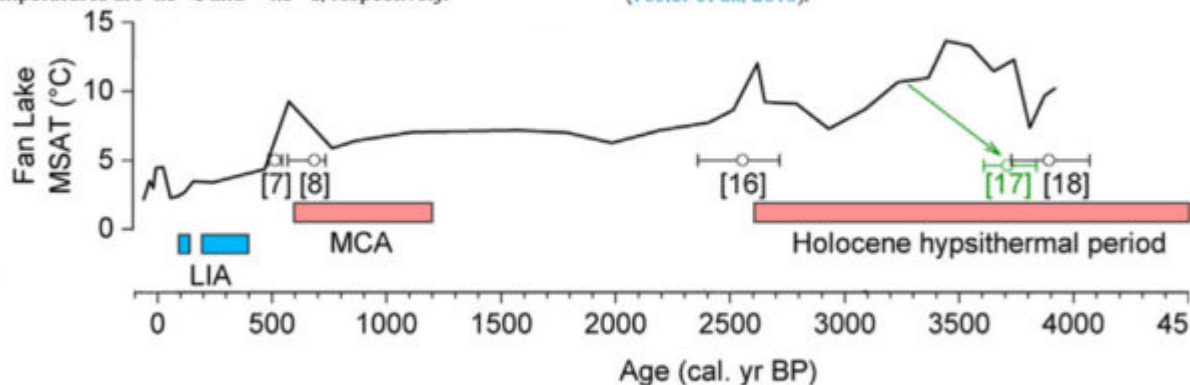
Ecological response of a glacier-fed peatland to late Holocene climate and glacier changes on subantarctic South Georgia

Zhengyu Xia ^{a,*,1}, Lea Toska Oppedal ^b, Nathalie Van der Putten ^c, Jostein Bakke ^b,
Zicheng Yu ^{a,d}



South Georgia has an overall cool oceanic climate. Weather station data are available from Grytviken (Fig. 1c) since 1905 CE. Based on data from the Global Historical Climatology Network (GHCN), the mean annual temperature is 1.9 °C and the mean summer (December–February) and winter (June–August) temperatures are 4.8 °C and –1.3 °C, respectively.

Although the biomarker-based paleotemperature proxy has been calibrated for modern temperature data of regional lakes, summer temperatures as high as 14 °C reconstructed from Fan Lake are outside the range of their modern calibration dataset in which the warmest site has a summer temperature of only 10 °C (Foster et al., 2016).



Mean summer air temperature (MSAT) record reconstructed from Fan Lake (Foster et al., 2016). Here the chronological anchor points for these temperature peaks used by Strother et al. (2015) are also shown along with their ID numbers (7, 8, 16, and 18). The green radiocarbon dating point (ID number 17) was rejected in the original age-depth model, but if used, the horizon of 3250 cal yr BP would be anchored to an older age, pulling this section of the MSAT curve rightward in the Bayesian age-depth modeling. The red horizontal bars below show the periods of past warm intervals by Foster et al. (2016) based on their multi-proxy dataset. MCA—Medieval Climate Anomaly.

The period of increased CARs could also be driven by climate warming. At Fan Lake, a biomarker-based summer temperature increase of 4 °C was inferred at around 600 cal yr BP (Fig. 4g), but other multi-proxy data in the same core documented this warming period earlier and formally from 1200 to 600 cal yr BP, referred to as the regional Medieval Climate Anomaly (Foster et al., 2016).

The CARs increased to as high as 140 g C m⁻² yr⁻¹ at 4000–3500 cal yr BP and 70 g C m⁻² yr⁻¹ at 3200–2700 cal yr BP when summer temperature was around 10 °C and 5 °C higher than present, respectively (Fig. 4f and g).

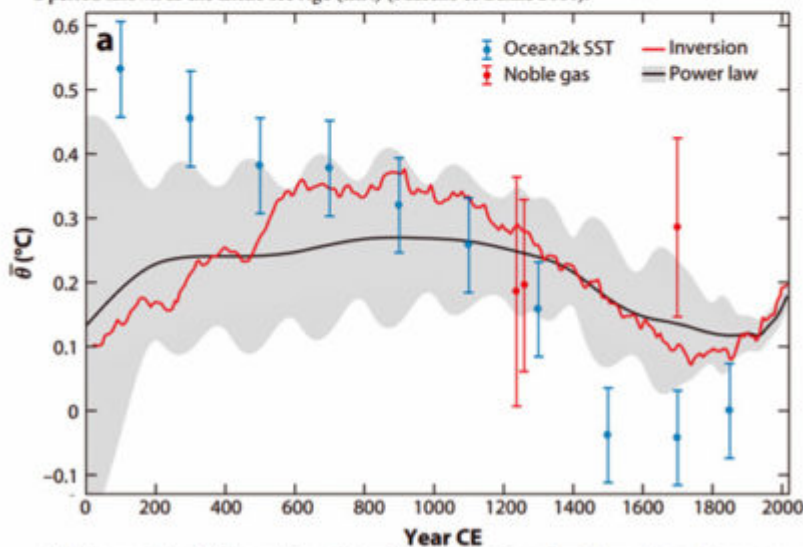
Gebbie, 2020: Die derzeitige Wärme in den Ozeanen beträgt nur etwa ein Drittel dessen, was zum Erreichen des Niveaus im Mittelalter erforderlich ist.

Annual Review of Marine Science / Volume 13, 2021 / Gebbie <https://doi.org/10.1146/annurev-marine-010419-010844>

Deglacial ocean uptake estimates vary from 12,000 to 20,000 ZJ (1 ZJ $\equiv 10^{21}$ J) and represent an awesome amount of energy that dwarfs the excess energy stored during the modern warming era by a factor of at least 20.

Early-twenty-first-century SST may already be warmer than MCA SST, but it is less likely that modern mean ocean temperature has surpassed MCA values. From the Gebbie & Huybers (2019) inversion, it was inferred that the MCA ocean stored 1,000 ZJ more than the ocean of the year 2000, and that the ~ 500 ZJ of heat uptake during the modern warming era is just one-third of what is required to reach MCA levels. Amplification of the high-latitude SST signal relative to the global mean can produce a greater MCA-LIA mean ocean cooling, which explains the greater MCA heat content relative to the present day. When considering the range of Common Era scenarios consistent with a power law, however, some cases are admitted where the MCA and the present day have similar oceanic heat content.

Marine proxy data compiled by the Ocean2k project (McGregor et al. 2015) indicate a global cooling trend after the peak of the MCA that reached its nadir over roughly the years 1400–1800, a period known as the Little Ice Age (LIA) (Paasche & Bakke 2010).



The Common Era. (a) The evolution of Ocean2k SST (blue circles, with $\sigma/2$ error bars) and mean ocean temperature, $\bar{\theta}$, as inferred from noble-gas measurements (red circles, with $\sigma/2$ error bars), the Gebbie & Huybers (2019) Common Era inversion (red line), and a power-law estimate (black line, with 2σ error shown in gray), referenced to global-mean SST in 1870.

[Die Studie liegt hinter einer Zahlsschranke. Anm. d. Übers.]

Wagner et al., 2020: Im Südosten von Grönland war es von den 1920er bis zu den 1940er Jahren wärmer als heute

Die kalten Jahrzehnte nach 1950 fallen mit der Großen Salzgehalts-Anomalie in den späten 60er bis frühen 70er Jahren zusammen, die durch die langfristige Abnahme des Index' der Nordatlantischen Oszillation (NAO) verursacht wurde und den Export von Süßwasser und Eis durch die Framstraße in die EGC [Ostgrönland-Strom] begünstigte (Dickson et al., 1996). Innerhalb von zwei bis drei Jahren erreichte die damit verbundene Salzgehalts-Anomalie die Labradorsee, was zu einer Reduktion der Konvektion und einer anschließenden Abschwächung der *Atlantic Meridional Overturning Circulation* (AMOC) führte. Dieser Mechanismus erklärt die niedrige Temperatur auf dem SE-Grönland-Schelf und die positive AMV während dieses Zeitraums (Ionita et al., 2016, Abbildung 6d). ... In der

alkSST-Aufzeichnung von Skjoldungen sowie in den CTD-Messungen vor Skjoldungen (Abbildung 5d) zeigt sich eine Rückkehr zu niedrigeren Temperaturen nach 2006, was auf die außergewöhnlich hohen Temperaturen um das Jahr 2000 hinweist. ... Unsere Studie zeigt, dass, obwohl die Schmelzwasserproduktion durch das Klima beeinflusst worden sein könnte, die Position des Gletscherrandes und das Kalben von Eisbergen im 20. Jahrhundert relativ konstant geblieben sind. Dies könnte auf die Lage des Gletschers mit einer begrenzten Eis-Ozean-Grenze und einem 90°-Zuflusswinkel zurückzuführen sein, der als Pinning-Punkt in seiner aktuellen Position wirkt. Unsere Studie veranschaulicht, dass die Wärme des Ozeans einen begrenzten Effekt auf einige Meeresschelfeis-Gletscher haben kann.

AGU ADVANCING EARTH AND SPACE SCIENCE
Paleoceanography and Paleoclimatology

Volume 25, Issue 2
 March 2020

Sea Surface Temperature Variability on the SE-Greenland Shelf (1796–2013 CE) and Its Influence on Thrym Glacier in Nørre Skjoldungesund

David J. Wagner, Marie-Alexandrine Sicre, Kristian K. Kjeldsen, John M. Jaeger, Anders A. Bjark, Flor Vermassen, Longbin Sha, Kurt H. Kjær, Vincent Klein, Camilla S. Andresen

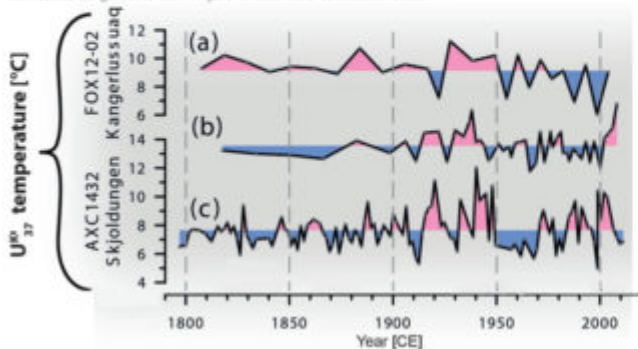
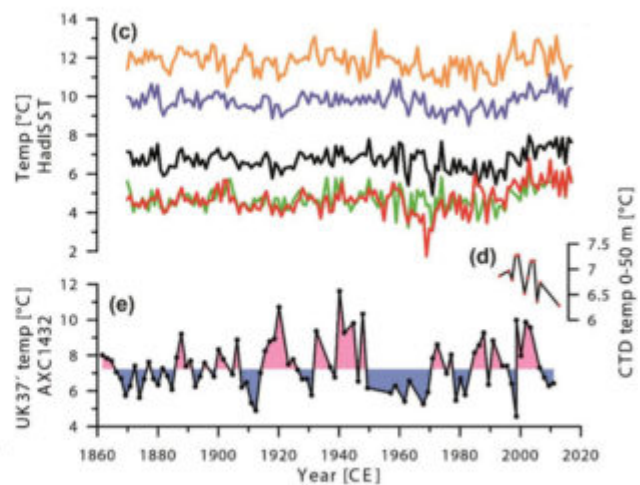


Figure 6: (a)-(c) AlkSST reconstructions from three fjords in SE-Greenland. (a) Kangerlussuaq Fjord, core FOX12-02 (Vermassen et al., 2019), (b) Sermilik Fjord, core ER07 (Andresen et al., 2017) and (c) Nørre Skjoldungesund, core AXC1432 (this study, using the BAYSPLINE calibration). Colors indicate the variance from the individual average.



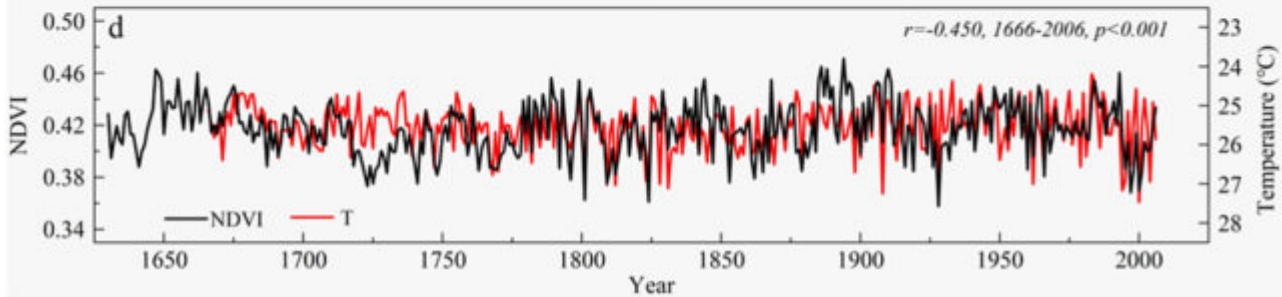
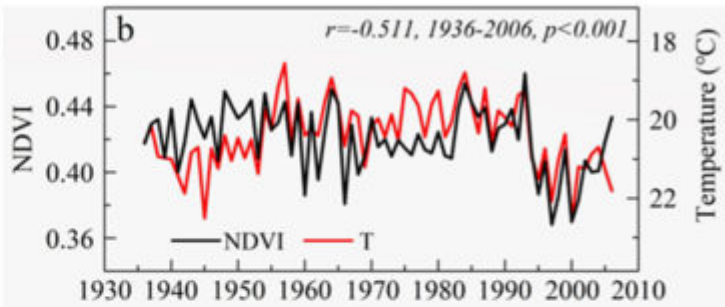
(c): Average July-October Hads SST temperature (Rayner et al., 2003), with the color code for each plot being related to the color of each box shown on the map in (a). (d): average CTD temperature within the uppermost 50 m from (b). (e): BAYSPLINE AlkSST record from Nørre Skjoldungesund starting in 1860. Colors indicate variation from the average value 7.23°C.

Sun et al., 2020: Keine Erwärmung in Nordwest-China seit dem 17. Jahrhundert, Abkühlung seit den 1950er Jahren



Tree-ring evidence of the impacts of climate change and agricultural cultivation on vegetation coverage in the upper reaches of the Weihe River, northwest China

Changfeng Sun ^{a, R.}, Yu Liu ^{a, b, c, R.}, Huiming Song ^{a, b, c}, Qiang Li ^{a, b, c}, Qiufang Cai ^{a, b, c}, Lu Wang ^a, Congxi Fang ^a, Ruoshi Liu ^a



Weckstrom et al., 2020: Abkühlung des nördlichen Nordatlantiks und zunehmendes Meereis seit den 1930er Jahren



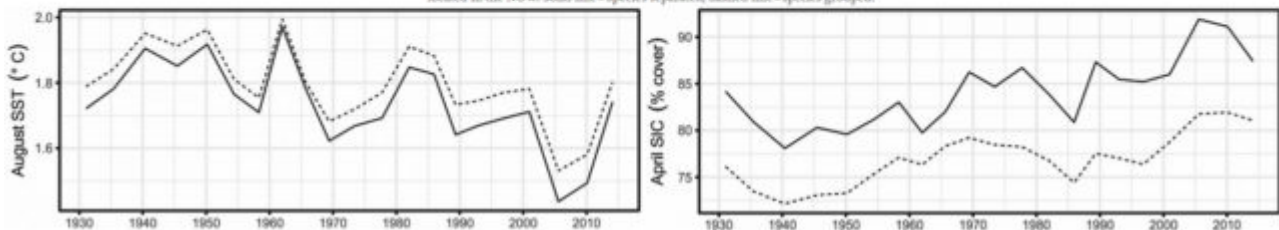
Improving the paleoceanographic proxy tool kit – On the biogeography and ecology of the sea ice-associated species *Fragilariopsis oceanica*, *Fragilariopsis reginae-jahniae* and *Fossula arctica* in the northern North Atlantic

Kaarina Weckström ^{a, b, c, R.}, Benjamin Redmond Roche ^{a, b, c}, Arto Miettinen ^a, Diana Kruczyk ^{a, b, c}, Audrey Linnegren ^a, Steve Juggins ^a, Sofia Ekelund ^a, Maja Heikkilä ^a

To define the relationship of the three species with their environment, we used August sea-surface temperature (aSST) and April sea-ice concentration (aSIC) for the numerical analyses. These have been found to be statistically significant variables (and months, i.e., August for SST and April for sea ice) in explaining diatom assemblage distribution in the North Atlantic (Bernier et al., 2008; Miettinen et al., 2015).

Species	Ecology & distribution
<i>Fragilariopsis oceanica</i>	Cold-water species abundant below 7°C, found at a variety of sea-ice concentrations (highest abundances at both <25% and >75% aSIC), preference for stratified waters (cold, fresh surface layer).
<i>Fragilariopsis reginae-jahniae</i>	MIZ species, related to generally high aSIC (highest abundances >75%), and cold aSST (highest abundances around 3°C), preference for stratified waters (cold, fresh surface layer).
<i>Fossula arctica</i>	Sea-ice species, related to high aSIC (highest abundances >75%) and cold aSST (optimum 2.6°C), preference for stratified waters (cold, fresh surface layer). Potential polynya species (affinity for higher nutrient availability).

Fig. 6. Quantitative reconstructions of past aSST and aSIC from core AMD15-CASQ1-BC located in the NOW. Solid line - Species separated, dashed line - species grouped.



Singh et al., 2020: Auf dem antarktischen Kontinent ist es während der letzten 7 Jahrzehnte nicht wärmer geworden.

Geringe kontinentale Klimasensitivität der Antarktis aufgrund hoher Eisschild-Orographie ... Der antarktische Kontinent hat sich in den

letzten sieben Jahrzehnten nicht erwärmt, trotz eines monotonen Anstiegs der atmosphärischen Konzentration von Treibhausgasen.

npj | climate and atmospheric science

Low Antarctic continental climate sensitivity due to high ice sheet orography

Hansi A. Singh & Lorenzo M. Polvani

npj Climate and Atmospheric Science 3, Article number: 39 (2020) | Cite this article

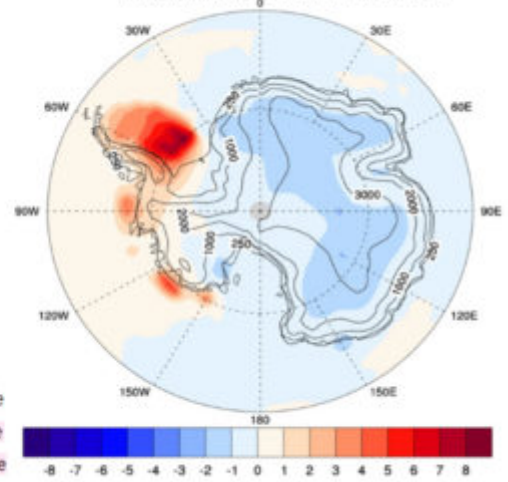
The Antarctic continent has not warmed in the last seven decades, despite a monotonic increase in the atmospheric concentration of greenhouse gases. In this paper, we investigate whether the high orography of the Antarctic ice sheet (AIS) has helped delay warming over the continent.

Our results suggest that the high elevation of the present AIS plays a significant role in decreasing the susceptibility of the Antarctic continent to CO₂-forced warming.

In the present study, we do find that the net (downward) surface longwave flux with CO₂-doubling is greater when Antarctic orography is flattened. However, we are leery to attribute the surface-amplified warming with flat orography to this factor: analysis of surface radiative kernels indicates that anomalies in the downward longwave flux at the surface primarily arise as a consequence of surface temperature anomalies, rather being the cause of those anomalies⁵⁶.

Fig. 1: Observed surface temperature anomaly.

Temperature (K), 1984-2014 minus 1950-1980



Mean surface temperature anomaly over years 1984-2014 (compared to the base period 1950-1980) over the Antarctic from the NOAA-MRCSST regrided temperature product⁵⁷. Contours show the surface elevation above sea level (in m).

Link:

<https://notrickszone.com/2021/01/14/what-global-warming-148-new-2020-scientific-papers-affirm-recent-non-warming-a-degrees-warmer-past/>

Übersetzt von Chris Frey EIKE